



Quantitative proteomic analysis reveals proteins involved in the neurotoxicity of marine medaka *Oryzias melastigma* chronically exposed to inorganic mercury



Yuyu Wang^{a,b}, Dazhi Wang^a, Lin Lin^a, Minghua Wang^{a,*}

^aKey Laboratory of the Ministry of Education for Coastal and Wetland Ecosystems, College of the Environment and Ecology, Xiamen University, Xiamen 361005, China

^bCenter for Environmental Health Research, South China Institute of Environmental Sciences, Ministry of Environmental Protection of the People's Republic of China, Guangzhou 510655, China

HIGHLIGHTS

- We investigated protein profiles of fish brain using 2D-DIGE analysis.
- Accumulation of Hg and the cellular ultrastructure of fish brain were examined.
- The results showed that Hg was significantly accumulated in the fish brain.
- Inorganic Hg caused noticeable damage to the fish brain.
- Multiple proteins and biological processes are involved in Hg neurotoxicity.

ARTICLE INFO

Article history:

Received 26 January 2014

Received in revised form 11 September 2014

Accepted 18 September 2014

Available online 15 October 2014

Handling Editor: J. de Boer

Keywords:

Inorganic mercury
Marine medaka
Neurotoxicity
Proteomics

ABSTRACT

Mercury is a ubiquitous environmental contaminant which exerts neurotoxicity upon animals. Nevertheless, the molecular mechanisms involved in inorganic mercury neurotoxicity are unknown. We investigated protein profiles of marine medaka, chronically exposed to mercuric chloride using two-dimensional difference gel electrophoresis (2D-DIGE) and matrix-assisted laser desorption/ionization tandem time-of-flight mass spectrometry (MALDI-TOF-TOF MS) analysis. The mercury accumulation and ultrastructure were also examined in the brain. The results showed that mercury was significantly accumulated in the treated brain, and subsequently caused a noticeable damage. The comparison of 2D-DIGE protein profiles between the control and treatment revealed that 16 protein spots were remarkably altered in abundance, which were further submitted for MALDI-TOF-TOF MS analysis. The identified proteins indicated that inorganic mercury may cause neurotoxicity through the induction of oxidative stress, cytoskeletal assembly dysfunction and metabolic disorders. Thus, this study provided a basis for a better understanding of the molecular mechanisms involved in mercury neurotoxicity.

© 2014 Elsevier Ltd. All rights reserved.

1. Introduction

Mercury is a ubiquitous environmental contaminant found in ocean and freshwater fish, shellfish, and plants, and it causes a wide range of adverse effects in humans (Ung et al., 2010). Mercury pollution originating from anthropogenic activities and industrialization has resulted in several catastrophes in Japan (Kudo et al., 1998), Iraq (Bakir et al., 1973) and the Amazon basin (Pfeiffer and Lacerda, 1988). Moreover, many high-risk sites have been identified in Asia (Li et al., 2009). Mercury pollution has become a worldwide public health concern.

* Corresponding author. Tel./fax: +86 592 2880219.

E-mail address: wmhyao2007@xmu.edu.cn (M. Wang).

In the environment, mercury exists in three forms possessing different bioavailability and toxicity: the metallic element, inorganic salts and organic compounds (Clarkson, 2002; Mousavi et al., 2011). Among them, methylmercury (MeHg) is considered to be the most toxic and has extensively been studied. MeHg can pass through the blood-brain barrier and accumulate in the central nervous system (CNS) in both humans and fish (Aschner et al., 2007; Clarkson and Magos, 2006), thus leading to neurological damage to the brain (Berntssen et al., 2003; Clarkson, 1997; Zheng et al., 2003). Moreover, MeHg also causes toxicity to the kidneys, as well as the CNS, and cardiovascular, gastrointestinal, and immune systems (Holmes et al., 2009; Virtanen et al., 2007). Several molecular and cellular mechanisms of MeHg toxicity have been postulated. However, so far, little is known concerning the

molecular mechanisms involved in the neurotoxicity caused by inorganic mercury, although inorganic mercury species are widely distributed in the environment (Fitzgerald, 2003; Goldman and Shannon, 2001). Guzzi and La Porta (2008) report that MeHg is slowly metabolized to inorganic mercury by the intestinal microflora, and elevated levels of inorganic mercury are found in the brains of humans, pups and monkeys exposed to MeHg (Davis et al. 1994; Ishitobi et al., 2010; Vahter et al., 1995). Thus, even after MeHg exposure, mercury toxicity to organisms might be ascribed to inorganic mercury attack, due to the conversion of MeHg to inorganic mercury. Furthermore, infants and children present a higher absorption rate of inorganic mercury compared to adults (Goyer and Clarkson, 2001; Walsh, 1982). Overall, it is very important to explore the molecular mechanisms of inorganic mercury neurotoxicity in organisms.

Two-dimensional fluorescence difference gel electrophoresis (2D-DIGE) is a newly developed quantitative proteomic approach, which directly labels lysine groups on proteins with cyanine CyDye DIGE Fluor minimal dyes prior to isoelectric focusing, enabling the labeling of 2–3 samples with different dyes and electrophoresis of all the samples on the same 2D-DIGE gel (Tannu and Hemby, 2006). 2D-DIGE has facilitated vital advances in the measurement of protein expression alterations in control and treatment samples. Recently this approach has been applied to investigate the toxicity mechanisms of several pollutants in aquatic organisms (Eyckmans et al., 2012; Roland et al., 2013).

In our study, marine medaka (*Oryzias melastigma*) were chronically exposed to different mercuric chloride (HgCl_2) concentrations (1 or $10 \mu\text{g L}^{-1}$) for 60 d, and the protein profiles of the brains of exposed and non-exposed medaka were analyzed using 2D-DIGE, and the differentially expressed protein spots were identified using matrix-assisted laser desorption/ionization tandem time-of-flight mass spectrometry (MALDI-TOF-TOF MS) analysis. In addition, the mercury content as well as cellular ultrastructural changes in the brain were also investigated. This study aimed to elucidate the mode-of-action of inorganic mercury neurotoxicity, and to identify potential protein biomarker candidates for aquatic environmental monitoring.

2. Materials and methods

2.1. Medaka exposure experiment

Medaka (*O. melastigma*) were acclimatized in aerated seawater tanks for 15 d prior to the experiment at a water temperature of 25°C under a 12 h light/dark cycle, and fed twice a day, 9:00 am and 3:00 pm, with commercial artemia dry bait. Then, fish (weighing $0.5 \pm 0.05 \text{ g}$) were randomly assigned to three experimental groups for exposure to two mercury treatments, 1 and $10 \mu\text{g L}^{-1}$, and non-exposure. Each treatment included two groups with 40 fish. The experiments were carried out in glass tanks ($44 \times 30 \times 28 \text{ cm}^3$) with 30 L filtered seawater water and lasted for 60 d under the same conditions as during acclimation described above. Each day half of the aged water was renewed with fresh seawater containing 1 or $10 \mu\text{g L}^{-1}$ HgCl_2 , or none. No mortality was found in the control and $1 \mu\text{g L}^{-1}$ -treated groups, but 5% were observed to be dead in the $10 \mu\text{g L}^{-1}$ treatment. At the end of exposure, the brains of 24 medaka (12 fish per tank) were dissected and pooled. Then the pooled tissues were randomly divided into three parts, and subjected to proteomic analysis, representing three independent replicates. For the mercury accumulation analysis, the brains of another 36 medaka (18 fish per tank) were collected and divided into three parts, concomitantly producing three replicates for each treatment. The remaining carcasses were fixed in 2.5% glutaraldehyde for cell ultrastructure analysis. It should be noted that the medaka used in this study were mixed-sex adult fish with the same age of six

months. All seawater used was filtered through $0.45 \mu\text{m}$ acetate fiber membranes, with the background concentration of total-mercury (T-Hg) being $0.0051 \mu\text{g L}^{-1}$. The seawater characteristics were described as follows: dissolved oxygen, $6.2\text{--}6.7 \text{ mg L}^{-1}$; salinity, 29–30 PSU; and pH, 8.0–8.1.

2.2. Mercury concentration analysis

T-Hg concentrations in the medaka brain were measured using the EPA 7474 method, with a few modifications. After freeze-drying for 2 d, the tissues were digested in 70% nitric acid in a heating block at 80°C overnight. In the hydrochloride/bromate/bromide mixture (Sigma–Aldrich), mercury was oxidized with stannous chloride (Wako) and analyzed using cold vapor atomic fluorescence spectrometry (CVAFS, Brooks Rand Model III). Standard reference materials (Mussel Homogenate IAEA 142 and Tuna Fish Flesh homogenate IAEA 436) were concurrently digested and measured for T-Hg, and the recoveries were $>90\%$ in the standards. The T-Hg content of the medaka brains was measured as ng g^{-1} dry weight (DW), and the data were expressed as mean values \pm standard deviation (SD).

2.3. Ultrastructure analysis

For ultrastructure analysis, fish brains were fixed in 2.5% glutaraldehyde in 0.1 M phosphate buffer (pH 7.3) for 3 h at 4°C . The fixed brains were washed three times using 0.1 M phosphate buffer (pH 7.3) at 20 min intervals with periodic agitation, then further fixed in 1% osmium tetroxide for 2 h at 4°C , followed by a phosphate buffer wash three times at 20 min intervals. After dehydration in alcohol, brains were embedded in Epon-Araldite. Ultra-thin sections ($50\text{--}80 \text{ nm}$) were moved onto titanium grids, stained with uranyl acetate and lead citrate and observed using a JEM 2100 Transmission Electron Microscope. Image analysis was conducted using the ImageJ 1.36 program (NIH, Washington, DC).

2.4. Proteomic analysis

2.4.1. Protein extraction

Frozen fish brains were suspended in 1 mL of 10% w/v trichloroacetic acid (TCA)/acetone for 1 h at 4°C . After centrifugation at 18000 g for 30 min at 4°C , the pellets were recovered and subsequently homogenized in 1.0 mL of 20% TCA/acetone (w/v) lysis buffer using an ultrasonic disrupter. The supernatant was removed by centrifugation at 18000 g for 30 min at 4°C , and the pellet was washed twice with 80% acetone (v/v) and twice with ice-cold acetone. The pellet was recovered by centrifugation at 18000 g for 30 min at 4°C each time. Residual acetone was removed in a SpeedVac for about 5 min. The pellet was dissolved in 120 μL rehydration buffer containing 30 mM Tris, 7 M urea, 2 M thiourea, and 4% CHAPS (Bio-Rad, USA). The solution was centrifuged at 20000 g for 30 min at 10°C and the supernatant was collected for 2D-DIGE analysis. Protein concentrations were quantified using the 2-D Quant kit (GE Healthcare).

2.4.2. CyDye labeling

The proteins were labeled with CyDyes for performing 2D-DIGE. Prior to protein labeling, the pH of the samples was checked with a pH indicator strip and, if necessary, the pH was adjusted to 8.5 using 50 mM NaOH. An internal standard was prepared by making a mixture with equal amounts of all the samples used in this experiment. The protein samples were labeled with Cy3 or Cy5 cyanine dye and the internal standard with Cy2 dye, by adding 400 pmol of CyDye per $50 \mu\text{g}$ protein. The labeling reaction was performed for 30 min on ice in the dark. Afterward, the reaction was quenched

with the addition of 1 μL 10 mM L-lysine (Sigma, USA) followed by incubation for 10 min on ice in the dark.

2.4.3. 2D-DIGE analysis

After labeling, the samples were combined according to the dye-swapping scheme, as shown in Table 1. The combined mixtures containing 150 μg protein were brought up to a final volume of 450 μL with 1 \times rehydration buffer, after which 0.5% IPG buffer 4–7 (GE healthcare, USA) was added and they were thoroughly mixed. The labeled samples were then applied to the strips on an Ettan IPGphor III Isoelectric Focusing System (GE Healthcare, USA). Isoelectric focusing was conducted for a total of 60 kV-h using the following conditions: 40 V for 5 h, 100 V for 6 h, gradient to 500 V in 30 min, gradient to 1000 V in 30 min, gradient to 2000 V in 1 h, gradient to 10000 V in 1 h, and finally 10000 V for 6 h. After the first dimension was run, each strip was equilibrated with about 10 mL equilibration buffer containing 50 mM Tris (pH 8.8), 6 M urea, 30% glycerol, 2% SDS, 1% DTT and a trace amount of bromophenol blue, for 17 min. The strip was then placed in fresh equilibration buffer containing 2.5% iodoacetamide (instead of DTT) for another 17 min. Subsequently an 11.5% SDS-PAGE second dimension was performed. Electrophoresis was carried out at 10 mA gel^{-1} for 15 min, followed by a 6 h run at 200 V until the bromophenol blue front reached the edge of the gels. The protein spot patterns of the three different dyes were acquired using an Ettan DIGE Imager laser scanner (GE Healthcare) at the excitation/emission wavelength of 488/520 nm (Cy2), 532/670 nm (Cy3), and 633/670 nm (Cy5). The exposure time of the laser was chosen in such a way that the protein spots had no saturated signal. After imaging for CyDye, the gels were further subjected to silver staining.

2.4.4. Data analysis

Image analysis was performed with the aid of the DeCyder version 6.5 suite (GE Healthcare, USA). First, protein spot detection and quantification compared with the internal standard as a volume ratio was performed with the Differential In-gel Analysis module. Second, protein spots on different gels were matched, and statistical analysis was carried out with the Biological Variation Analysis module. The one-way ANOVA test ($P < 0.05$) was used to pick out the significant differentially expressed protein spots among the groups. When the spots were selected to be significant, they were carefully checked for correct matching throughout all the gels and were included in the pick list. The fold changes of treatment/control were calculated based on their differences in standardized abundance.

2.4.5. Silver staining

Silver staining was performed following the method of Wang et al. (2010). Briefly, the gel was fixed for 2 h initially in a fixation solution containing 40% (v/v) ethanol and 10% (v/v) acetic acid. It was then sensitized in a solution containing 30% (v/v) ethanol, 0.2% (w/v) sodium thiosulphate, 6.8% (w/v) sodium acetate and

0.125% (v/v) glutaraldehyde, followed by three Milli-Q water washes (5 min each time). Then the gel was stained for 20 min in 0.25% (w/v) silver nitrate with 0.015% (v/v) formaldehyde and washed twice with Milli-Q water (0.5 min each time). The gel was developed in 2.5% (w/v) sodium carbonate containing 0.0074% (v/v) formaldehyde. The reaction was stopped with 1.5% (w/v) ethylenediaminetetraacetic acid, disodium salt.

2.4.6. Mass spectrometric analysis

The altered protein spots were manually excised from 2-DE gels. The gel pieces were washed with buffer containing 25 mM ammonium bicarbonate in 50% acetonitrile (ACN), destained with 30 mM potassium ferricyanide and 100 mM sodium thiosulfate, and washed again with 25 mM ammonium bicarbonate in 50% ACN. After dehydration with 100% ACN, the dry gel pieces were digested by adding 10.0 $\text{ng } \mu\text{L}^{-1}$ trypsin (Promega, Madison, WI) in 10 mM ammonium bicarbonate overnight at 37 °C. For MALDI-TOF/TOF MS analysis, 1 μL of the digest mixture was mixed on-target with 0.5 μL of 100 mM α -cyano-4-hydroxy-cinnamic acid in 50% ACN and 0.1% trifluoroacetic acid on the target plate before being dried and analyzed with a MALDI-TOF/TOF mass spectrometer (5800 Proteomics Analyzer, Applied Biosystems, Foster City, CA). MALDI-TOF MS and TOF-TOF tandem MS were performed and data were acquired in the positive MS reflector mode with a scan range from 900 to 4000 Da, and five monoisotopic precursors ($S/N > 200$) were selected for MS/MS analysis. For interpretation of the mass spectra, a combination of peptide mass fingerprints and peptide fragmentation patterns was used for protein identification in an NCBI nonredundant database using the Mascot search engine (<http://www.matrixscience.com>). All mass values were considered monoisotopic, and the mass tolerance was set at 75 ppm. One missed cleavage site was allowed for trypsin digestion; cysteine carbamidomethylation was assumed as a fixed modification, and methionine was assumed to be partially oxidized. Results with C.I.% (Confidence Interval%) values greater than 95% were considered to be a positive identification. The identified proteins were then matched to specific processes or functions by searching Gene Ontology (<http://www.geneontology.org/>).

2.5. Statistical tests

All measurements were replicated at least three times and the data were expressed as mean values \pm standard deviation (SD). Statistical analysis was carried out using a one-way ANOVA or an independent-samples t-test to evaluate whether the means were significantly different among the groups. Significant differences were indicated at $P < 0.05$. Prior to one-way ANOVA, data were log transformed to meet ANOVA assumptions of normality and variance homoscedasticity.

3. Results

3.1. Mercury accumulation in the medaka brain

After exposure to HgCl_2 for 60 d, the medaka brain was subjected to T-Hg content analysis. T-Hg concentration in the brain of unexposed medaka was $163.8 \pm 13.2 \text{ ng g}^{-1} \text{ DW}$. However, the presence of HgCl_2 significantly enhanced mercury accumulation in the mercury-exposed medaka brains (Fig. 1; $P < 0.001$), i.e. the T-Hg contents reached 8582.9 ± 168.7 and $12329.4 \pm 287.9 \text{ ng g}^{-1} \text{ DW}$ in the medaka brains exposed to 1 and 10 $\mu\text{g L}^{-1} \text{ HgCl}_2$, respectively.

3.2. Effects of HgCl_2 on cellular ultrastructure in the medaka brain

The ultrastructure of medaka brain chronically exposed to HgCl_2 is shown in Fig. 2. The results showed that the neurocyte of

Table 1
Experimental design for the 2D-DIGE proteome profiling.

Gel	Cy2	Cy3	Cy5
1	Internal standard	Control 1	Low treatment 1
2	Internal standard	High treatment 1	Control 2
3	Internal standard	Low treatment 2	Control 3
4	Internal standard	Control 4	High treatment 2
5	Internal standard	Low treatment 3	High treatment 3

Note: At least three replicate samples for each group (control, 1 and 10 $\mu\text{g L}^{-1}$ mercury treatments) were used and labeled with Cy3 or Cy5. Each gel contained an internal standard and two samples. The 1 and 10 $\mu\text{g L}^{-1}$ mercury treatments were assigned as low and high treatments respectively.

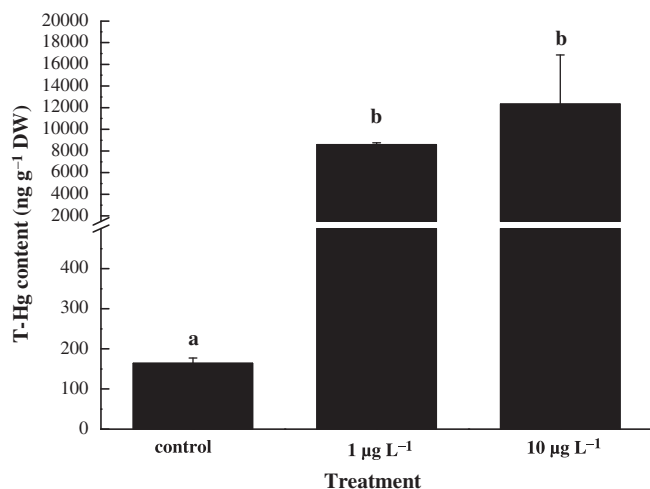


Fig. 1. Total-mercury (T-Hg) content in the brain tissue of the medaka *Oryzias melastigma* after 60 d exposure to different mercury chloride (HgCl_2) concentrations (control, 1 and 10 $\mu\text{g L}^{-1}$). Data are expressed as mean values \pm SD ($n = 3$). Different letters indicate a statistically significant difference at $P < 0.05$.

unexposed medaka contained few cisternae in the cell. Meanwhile, the well-shaped organelles were evenly distributed in the cellular cytoplasm (Fig. 2A). Numerous ribosomes as well as mitochondria were found in the cells. However, after 60 d exposure, widespread cisternae were observed in the cytoplasm, with dilation or even vesiculation, especially in the medaka brain exposed to 10 $\mu\text{g L}^{-1}$ HgCl_2 . Ridge disappearance and swelling of the mitochondria were also observed in the treatment. In the control, myelinated nerve fibers were tightly packed, slender and uniform-shaped (Fig. 2B). However, the arrangement of the myelinated nerve fiber in the

mercury exposed medaka brain became loose and a large number of separated nodes of Ranvier directly induced discontinuation of the nerve fibers.

3.3. 2D-DIGE analysis of differential protein expression

In total, nine samples were obtained in this study (three biological replicates per group). After being labeled with Cy3 or Cy5, the samples were run in five gels together with an internal standard labeled with Cy2 (Table 1). The internal standard represented an average of all the samples which were compared, and was used as a normalization standard across all gels. A representative 2D-DIGE image is shown in Fig. 3. More than 600 protein spots could be matched with all the images. Among them, a total of 16 significantly differentially expressed protein spots were detected with a one-way ANOVA test ($P < 0.5$ with differences of ≥ 1.5 in expression). Among them, eight protein spots were significantly up-regulated in the mercury exposed medaka, while the other eight were down-regulated.

3.4. Identification of the differentially expressed proteins in the medaka brain

All the differentially expressed protein spots were submitted for identification using MALDI-TOF-TOF MS analysis and searched in the NCBI medaka database. Meanwhile, the protein spots which could not be identified from the medaka fish database were searched against the NCBI fish database. Consequently, 11 protein spots were successfully identified with C.I.% values higher than 95% (Table 2). Of them, four oxidative stress proteins including glutathione S-transferase (GST, spot 5), peroxiredoxin-1 (spots 3 and 6), and peroxiredoxin-1-like (spot 4) were up-regulated after mercury exposure. Three proteins involved in metabolism were markedly down-regulated under mercury treatment, and these were vacuolar

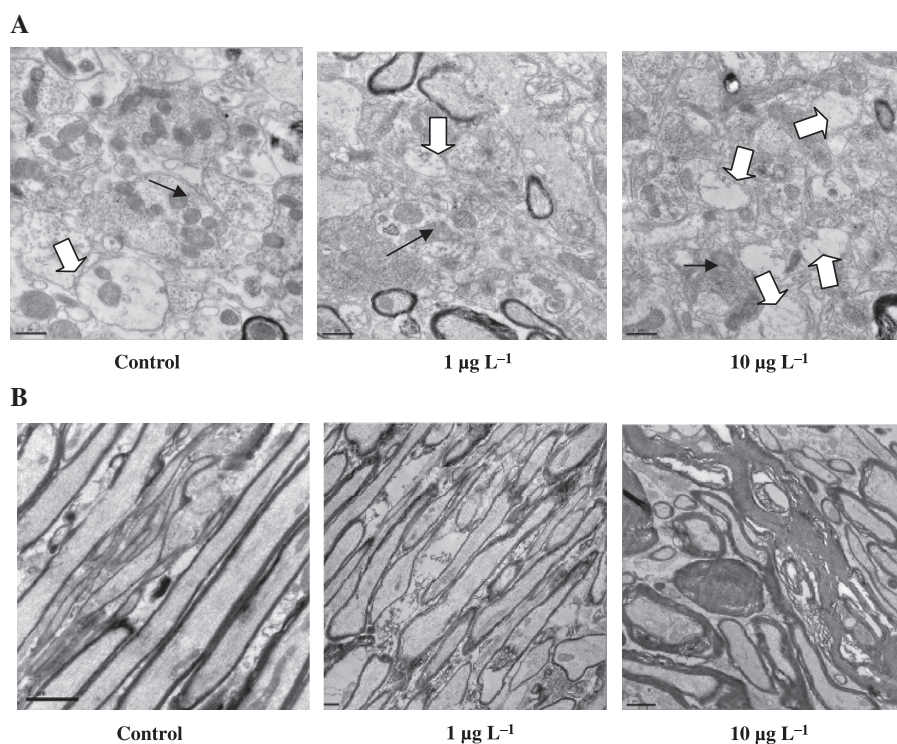


Fig. 2. Transmission electron micrographs of brain cells of the medaka *Oryzias melastigma* after 60 d exposure to different mercury chloride (HgCl_2) concentrations (control, 1 and 10 $\mu\text{g L}^{-1}$). (A) Mitochondria (black arrow) and cisternae (white arrow). (B) Myelinated nerve fiber.

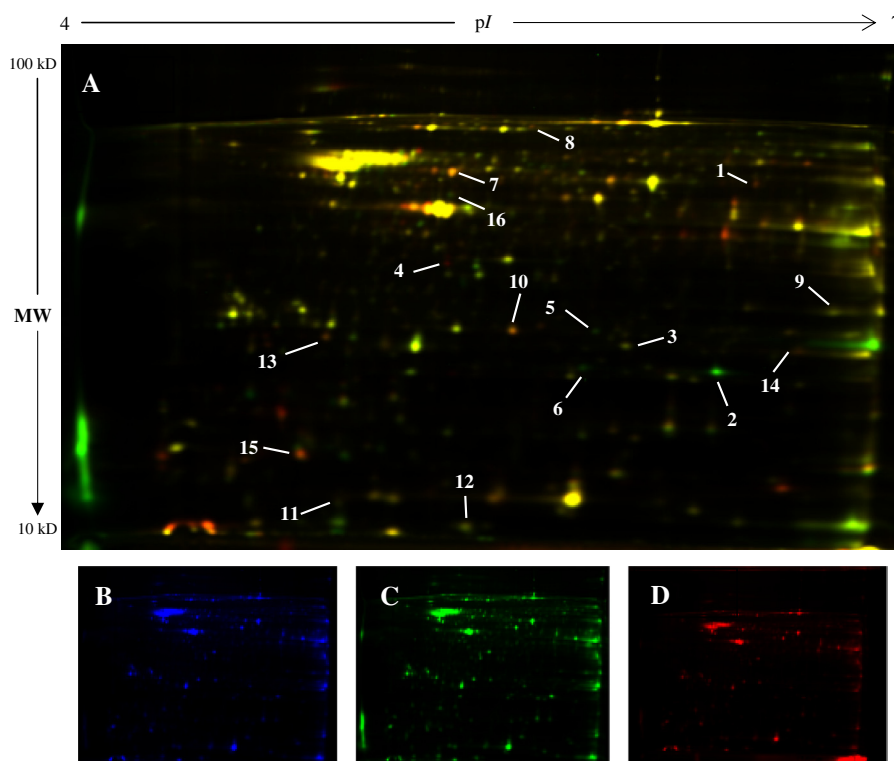


Fig. 3. Representative proteome map of the differentially expressed proteins in medaka *Oryzias melastigma* brain. (A) The labeled proteins were visualized for all of the fluorophores, and the differentially expressed protein spots are marked with numbers. (B) Cy2 represents mixing equal amounts of all the proteins as the internal standard. (C) Cy3 indicates the protein sample of the treated group. (D) Cy5 indicates the protein sample of the control group.

ATP synthase catalytic subunit A (spot 8), cytosolic nonspecific dipeptidase-like (spot 7) and glutamate carboxypeptidase-like protein (spot 9). Interestingly, four proteins were concerned with cytoskeletal assembly. Namely, beta-actin (spot 1), actin, cytoplasmic 1 (spot 10), and si:dkeyp-113d7.4 (spot 15) were consistently depressed under mercury treatment; however, myosin light chain 2 (spot 2) was increased in expression.

4. Discussion

Most studies are devoted to the nephrotoxicity of inorganic mercury in various aquatic organisms because inorganic mercury is mostly accumulated in the kidney (Goering et al., 2000; Rana, 2008; Risher and De Rosa, 2007; Zalups, 2000). However, the present study showed that high concentrations of mercury could be accumulated in the brain after mercury exposure, which is in line with previous studies that mercury evidently accumulates in the brain under mercury chloride treatment (Agarwal and Behari, 2007; Danscher et al., 1990; Hahn et al., 1990; Monteiro et al., 2010; Nylander and Weiner 1991; Yasutake et al., 2004). In our study, mercury treatment caused noticeable damage to the medaka brain, i.e. the ridge disappearance and swelling of the mitochondria, as well as the discontinuation of the nerve fiber into a large number of separated nodes of Ranvier being observed in the treated brain. Similarly, a study shows that nerves display disorganized disposition of axons and mainly disruption and dissociation of myelin sheaths in the brain of *Trichomycterus brasiliensis* after exposure to inorganic mercury (Oliveira Ribeiro et al., 1996). Obvious ultrastructural changes are also observed in the brain cortex of rats due to inorganic mercury toxicity (Gajkowska et al., 1992). Taken together, our study demonstrated that the brain is an important target organ of inorganic mercury and the exposure of inorganic mercury might cause neurotoxicity to medaka.

Inorganic mercury has a great affinity for the SH groups of endogenous biomolecules, reaching into the cells and tissues attached to thiol-containing proteins and low-molecular-weight thiols (Perottoni et al., 2004), and hence affecting the expression of various proteins (Agarwal and Behari, 2007). Proteomic analysis showed that inorganic mercury caused a significant alteration of protein profiles in medaka brain, and the proteins involved in oxidative stress, cytoskeletal assembly and macromolecular metabolism were significantly affected by HgCl₂ toxicity.

Peroxiredoxins play an important role in the removal of reactive oxygen species (ROS), thus minimizing their deleterious effects (Radyuk et al., 2001). GST plays a critical role in the defense against oxidative stress induced by cell injury (Sheehan et al., 1991), since it catalyzes the conjugation of glutathione with a variety of electrophilic compounds, including products resulting from oxidative damage in biological membranes and macromolecules (Beckett and Hayes, 1993; Carmagnol et al., 1981; Guemouri et al., 1991). There is evidence that in the presence of hydroxide, GST may play a role as glutathione reductase to increase reduced glutathione content, hence reducing the cell damage generated by the ROS (Marrs, 1996). Moreover, brain GST is mainly found in the glial compartment and in neurons (Cammer et al., 1989; Johnson et al., 1993). The above proteins provide a major intracellular defense against mercury-induced neurotoxicity (James et al., 2005). Consequently, the upregulation of peroxiredoxin-1, peroxiredoxin-1-like and GST in the brain might effectively cooperate to fight against excess ROS production caused by mercury toxicity, considering that the brain is especially vulnerable to free radical-induced damage because of its high oxygen consumption, abundant lipid content, and a limited amount of antioxidant capacity (Hasan et al., 2011). Previous studies also demonstrate that antioxidant systems have significantly been affected by MeHg exposure, being attributed to mercury-induced ROS overproduction (Gatti

Table 2
A detailed list for protein spots identified from the brain of medaka *Oryzias melastigma* following HgCl₂ exposure using MALDI-TOF/TOF MS.

Spot id.	Protein identity	Accession number	MASCOT score (peptides)	Protein score C.I.%	MW/pI	Organism	Molecular function	Fold change	
								1 µg L ⁻¹	10 µg L ⁻¹
<i>Cytoskeletal assembly</i>									
1	Beta-actin	gi 45505238	70(5)	99.998	15910.8/4.99	<i>Ictalurus punctatus</i>	Structural molecule activity	-1.31	-1.69
2	Myosin light chain 2	gi 60685065	133(5)	100	18437.2/4.75	<i>Oryzias latipes</i>	Structural molecule activity	3.26	3.76
10	Actin, cytoplasmic 1	gi 157278351	145(8)	100	41738.7/5.3	<i>Oryzias latipes</i>	Structural molecule activity	-1.84	-1.88
15	Si:dkkeyp-113d7.4	gi 167234796	79(8)	100	49903.8/4.94	<i>Danio rerio</i>	Structural molecule activity	-1.26	-2.60
<i>Oxidative stress</i>									
3	Peroxiredoxin-1	gi 327358437	79(3)	99.968	22055.2/6.3	<i>Oryzias melastigma</i>	Antioxidant activity	3.26	3.76
4	Peroxiredoxin-1-like	gi 432914796	854(14)	100	20078.3/5.37	<i>Oryzias latipes</i>	Antioxidant activity	1.05	2.00
5	Glutathione S-transferase	gi 110180509	59(2)	100	8067.9/5.42	<i>Oryzias javanicus</i>	Transferase activity	1.29	1.58
6	Peroxiredoxin-1	gi 327358437	60(3)	97.304	22055.2/6.3	<i>Oryzias melastigma</i>	Antioxidant activity	2.98	3.67
<i>Respiratory metabolism</i>									
7	Cytosolic nonspecific dipeptidase-like	gi 432950957	103(6)	100	53170.8/5.32	<i>Oryzias latipes</i>	Dipeptides hydrolase activity	-1.38	-1.57
8	Vacuolar ATP synthase catalytic subunit A	gi 209150762	118(10)	100	68669.9/5.37	<i>Salmo salar</i>	Transporter activity	-1.28	-1.67
9	Glutamate carboxypeptidase-like protein 1	gi 30349204	192(5)	100	20372.6/9.44	<i>Oreochromis mossambicus</i>	Carboxypeptidase activity	-1.08	-2.14

Note: MW represents molecular weight with pI for isoelectric point. Variations were calculated as treated/control spot volume ratio and if the result was below 1, it is reported as - control/treated ratio.

et al., 2004; Ni et al., 2010). Overall, inorganic mercury toxicity resulted in ROS overproduction and concomitant oxidative stress in the brain, indicating that inorganic mercury caused neurotoxicity mainly through oxidative stress in the brain.

In our study, three proteins associated with metabolism in fish brain: vacuolar ATP synthase catalytic subunit A, glutamate carboxypeptidase-like protein 1 and cytosolic nonspecific dipeptidase-like were identified. Vacuolar ATP synthase catalytic subunit A was down-regulated in mercury-exposed medaka brain, highlighting that mercury might inhibit the enzymes responsible for ATP synthesis in the mitochondria and subsequently lead to mitochondrial dysfunction. The brain is an energy-demanding organ where the processes related to signaling, especially propagation of the action potential, require the largest proportion of brain energy utilization (Siegel et al., 2006). Therefore, a decreased ATP level might undermine the ability of the brain cells to meet their energy requirements, and concomitantly to induce cell death and brain injury. Glutamate is the major excitatory neurotransmitter and plays key roles in development, learning, memory and response to injury (Featherstone, 2010). However, a high concentration of glutamate at the synaptic cleft acts as a toxin, inducing neuronal injury and death (Meldrum, 2000; Ozawa et al., 1998). Here, the down-regulation of glutamate carboxypeptidase-like protein 1 indicated that the hydrolysis of glutamate peptide bond was disturbed by mercury attack. In other words, inorganic mercury might enhance glutamate release, lead to elevated extracellular glutamate levels, and subsequently increase the influx of Ca²⁺ into postsynaptic neurons, finally producing several toxic events, e.g. dysfunction of calcium-dependent homeostatic mechanisms (Johnston, 2005), activation of cell death pathways and dysfunction of mitochondria (Hidalgo and Donoso, 2008). Glutamate dyshomeostasis has severe adverse effects on brain function. It is postulated that the dyshomeostasis of glutamate might be one of the upstream mechanism in mitochondrial dysfunction. Moreover, our results were consistent with the previous studies showing that MeHg exposure increases extracellular glutamate levels (Brookes and Kristt, 1989; Aschner et al., 2000; Porciuncula et al., 2003), and there might be some similarity between organic and inorganic mercury neurotoxicity.

Cytoskeletal structure takes an important role in the nervous system, since neurons exhibit characteristic cell shapes closely connected to their function and development, hence cytoskeletal disruptions being frequent hallmarks of neuropathology and neurodegenerative conditions (Brown and Bridgman, 2004; Siegel et al., 2006). Four proteins involved in cytoskeletal assembly were significantly affected by mercury. Actin is one of the highly conserved and most abundant proteins in the nervous system and forms a framework in neuronal cells, which plays roles in various types of cell motility, axonal morphogenesis, collateral branching, branch retraction, and axonal regeneration (Ishikawa and Kohama, 2007; Letourneau, 2009). Notably, actin is redox-sensitive and also actin-glutathionylation frequently occurred under conditions of oxidative stress (Dalle-Donne et al., 2003; Sakai et al., 2012). The down-regulation of beta-actin and actin cytoplasmic 1 highlighted an increased cell damage in the brain due to mercury attack, which might be exemplified by our ultrastructure analysis. Myosin (another important modulator of the cytoskeleton) has been recognized as a group of motor proteins that generate mechanical force by hydrolyzing ATP and interacting with actin filaments, and the power thus obtained is used in a wide variety of cellular functions in the developing nervous system, including neuronal migration, process outgrowth and growth cone motility, as well as other aspects of morphological changes of dendritic spines, axonal transport, vesicle transport and synaptic sensory functions (Brown and Bridgman, 2004; Ishikawa and Kohama, 2007). The up-regulation of myosin light chain 2 in the brain might be a

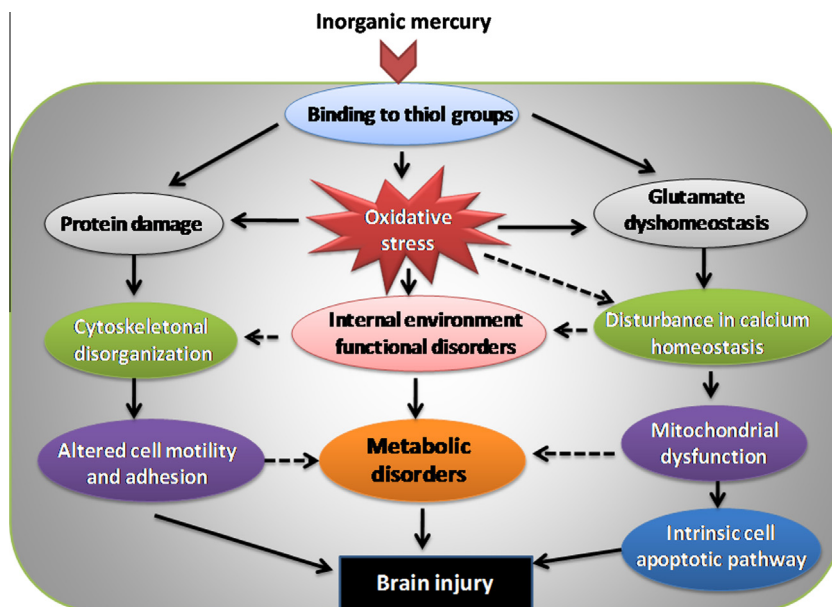


Fig. 4. The proposed scheme illustrating cellular events in brain tissue of medaka fish resulting from inorganic mercury toxicity.

compensatory reaction to instability of the actin cytoskeleton due to mercury toxicity. Moreover, it is suggested that myosin light chain 2 is not only a component of each myosin molecule (Collins et al., 1986), but also a member of the superfamily of Ca^{2+} -binding proteins (Moncrief et al., 1990), hinting an importance of calcium homeostasis in inorganic mercury neurotoxicity.

5. Conclusions

This study aimed to investigate, for the first time, the proteome of medaka brain exposed to inorganic mercury and to provide new insights into the molecular mechanism concerning inorganic mercury-induced neurotoxicity. The results showed that mercury was able to accumulate in the brain, and caused damage to the cellular ultrastructure of the medaka brain. Proteomic analysis demonstrated that proteins involved in oxidative stress, cytoskeletal disruptions and energy metabolism dysregulation were significantly affected by inorganic mercury, suggesting that inorganic mercury resulted in the neurotoxicity mainly through oxidative stress, cytoskeletal assembly dysfunction and metabolic disorders in the medaka brain (Fig. 4). It seems that inorganic mercury neurotoxicity is complex and diverse, and that multiple proteins and biological processes are involved. We noticed that the proteomic response in this study showed some similarity with that in the medaka brain acutely exposed to HgCl_2 in our previous work (Wang et al., 2011), i.e. the major cellular processes affected by inorganic mercury toxicity were similar in terms of their general functional categories (e.g. cytoskeletal assembly, oxidative stress, and energy metabolism). However, most of the individual proteins were different, highlighting that the toxic mechanisms caused by acute or chronic mercury attack were different. It should also be noted that several protein spots were definitely identified as the same protein (i.e. spots 3 and 6 for peroxiredoxin-1), and these proteins are likely to be protein isoforms. Protein isoforms can arise from alternative mRNA splicing and various post-translational modifications, such as cleavage, phosphorylation, acetylation, and glycosylation.

Acknowledgements

This work was supported by the National Natural Science Foundation of China (Nos. 40806051 and 41476094). The authors appreciate the kind help of Dr. Wen-Xiong Wang and Ke Pan

(The Hong Kong University of Science & Technology) in mercury analysis. Professor John Hodgkiss (The University of Hong Kong) is thanked for polishing the English in this manuscript.

References

- Agarwal, R., Behari, J.R., 2007. Role of selenium in mercury intoxication in mice. *Ind. Health* 45, 388–395.
- Aschner, M., Yao, C.P., Allen, J.W., Tan, K.H., 2000. Methylmercury alters glutamate transport in astrocytes. *Neurochem. Int.* 37, 199–206.
- Aschner, M., Syversen, T., Souza, D.O., Rocha, J.B., Farina, M., 2007. Involvement of glutamate and reactive oxygen species in methylmercury neurotoxicity. *Braz. J. Med. Biol. Res.* 40, 285–291.
- Bakir, F., Damluji, S.F., Amin-Zaki, L., Murtadha, M., Khalidi, A., al-Rawi, N.Y., Tikriti, S., Dahahir, H.I., Clarkson, T.W., Smith, J.C., Doherty, R.A., 1973. Methylmercury poisoning in Iraq. *Science* 181, 230–241.
- Beckett, G.J., Hayes, J.D., 1993. Glutathione-S-transferase: biomedical applications. *Adv. Clin. Chem.* 30, 282–380.
- Berntssen, M.H.G., Aatland, A., Handy, R.D., 2003. Chronic dietary mercury exposure causes oxidative stress, brain lesions, and altered behaviour in Atlantic salmon (*Salmo salar*) parr. *Aquat. Toxicol.* 65, 55–72.
- Brookes, N., Kristt, D.A., 1989. Inhibition of amino acid transport and protein synthesis by HgCl_2 and methylmercury in astrocytes: selectivity and reversibility. *J. Neurochem.* 53, 1228–1237.
- Brown, M.E., Bridgman, P.C., 2004. Myosin function in nervous and sensory systems. *Neurobiology* 58, 118–130.
- Cammer, W., Tansey, E., Abramovitz, M., Ishigaki, S., Listowski, I., 1989. Differential localization of glutathione-S-transferases Yp and Yb subunits in oligodendrocytes and astrocytes of rat brain. *J. Neurochem.* 52, 876–883.
- Carmagnol, F., Sinet, P.M., Rapin, J., Jerome, H., 1981. Glutathione-S-transferase of human red blood cells, assay, values in normal subjects, and in two pathological circumstance: Hyperbilirubinemia, and impaired renal function. *Clin. Chim. Acta* 117, 209–217.
- Clarkson, T.W., 1997. The toxicology of mercury. *Crit. Rev. Clin. Lab. Sci.* 34, 369–403.
- Clarkson, T.W., 2002. The three modern faces of mercury. *Environ. Health Perspect.* 110, 11–23.
- Clarkson, T.W., Magos, L., 2006. The toxicology of mercury and its chemical compounds. *Crit. Rev. Toxicol.* 36, 609–662.
- Collins, J.H., Theibert, J.L., Dalla Libera, L., 1986. Amino acid sequence of rabbit ventricular myosin light chain-2: identity with the slow skeletal muscle isoform. *Biosci. Rep.* 6, 655–661.
- Dalle-Donne, I., Rossi, R., Giustarini, D., Colombo, R., Milzani, A., 2003. Actin S-glutathionylation: evidence against a thiol-disulphide exchange mechanism. *Free Radic. Biol. Med.* 35, 1185–1193.
- Danscher, G., Horsted-Bindslev, P., Rungby, J., 1990. Traces of mercury in organs from primates with amalgam fillings. *Exp. Mol. Pathol.* 52, 291–299.
- Davis, L.E., Kornfeld, M., Mooney, H.S., Fiedler, K.J., Haaland, K.Y., Orrison, W.W., Cernichiar, E., Clarkson, T.W., 1994. Methylmercury poisoning: long-term clinical, radiological, toxicological, and pathological studies of an affected family. *Ann. Neurol.* 35, 680–688.

- Eyckmans, M., Benoot, D., Van Raemdonck, G.A., Zegels, G., Van Ostade, X.W., Witters, E., Blust, R., De Boeck, G., 2012. Comparative proteomics of copper exposure and toxicity in rainbow trout, common carp and gibel carp. *Comp. Biochem. Physiol. Part D Genom. Proteom.* 7, 220–232.
- Featherstone, D.E., 2010. Intercellular glutamate signaling in the nervous system and beyond. *ACS Chem. Neurosci.* 1, 4–12.
- Fitzgerald, W.F., 2003. Geochemistry of mercury in the environment. In: Lollar, B.S. (Ed.), *In Environmental Geochemistry, Treatise on Geochemistry*, vol. 9. Elsevier-Pergamon, Oxford, pp. 107–148.
- Gajkowska, B., Szumanska, G., Gadamski, R., 1992. Ultrastructural alterations of brain cortex in rat following intraperitoneal administration of mercuric chloride. *J. Hirnforsch.* 33, 471–476.
- Gatti, R., Belletti, S., Uggeri, J., Vettori, M.V., Mutti, A., Scandroglio, R., Orlandini, G., 2004. Methylmercury cytotoxicity in PC12 cells is mediated by primary glutathione depletion independent of excess reactive oxygen species generation. *Toxicology* 204, 175–185.
- Goering, P.L., Fisher, B.R., Noren, B.T., Papaconstatinou, A., Rojko, J.L., Marler, R.J., 2000. Mercury induces regional and cell-specific stress protein expression in rat kidney. *Toxicol. Sci.* 53, 447–457.
- Goldman, L.R., Shannon, M.W., 2001. Technical report: mercury in the environment: implications for pediatricians. *Pediatrics* 108, 197–205.
- Goyer, R.A., Clarkson, T.W., 2001. Toxic effects of metals. In: Klaassen, C.D. (Ed.), *Casarett & Doull's Toxicology: The Basic of Poisons*, sixth ed. McGraw Hill, NY, pp. 822–826.
- Guemouri, L., Artur, Y., Herbeth, B., Jeandel, C., Cuny, G., Siest, G., 1991. Biological variability of superoxide dismutase, glutathione peroxidase and catalase in blood. *Clin. Chem.* 37, 1932–1941.
- Guzzi, G., La Porta, C.A., 2008. Molecular mechanisms triggered by mercury. *Toxicology* 244, 1–12.
- Hahn, L.J., Kloiber, R., Leininger, R.W., Vimy, M.I., Lorscheider, F.L., 1990. Whole-body imaging of the distribution of mercury released from dental fillings into monkey tissues. *FASEB J.* 4, 3256–3260.
- Hasan, S., Bilal, N., Naqvi, S., Ashraf, G.M., Suhail, N., Sharma, S., Banu, N., 2011. Multivitamin-mineral and vitamins (E + C) supplementation modulate chronic unpredictable stress-induced oxidative damage in brain and heart of mice. *Biol. Trace Elem. Res.* 142, 589–597.
- Hidalgo, C., Donoso, P., 2008. Crosstalk between calcium and redox signaling: from molecular mechanisms to health implications. *Antioxid. Redox Signal.* 10, 1275–1312.
- Holmes, P., James, K.A., Levy, L.S., 2009. Is low-level environmental mercury exposure of concern to human health. *Sci. Total Environ.* 408, 171–182.
- Ishikawa, R., Kohama, K., 2007. Actin-binding proteins in nerve cell growth cones. *J. Pharmacol. Sci.* 105, 6–11.
- Ishitobi, H., Sander Stern, S., Thurston, S.W., Zareba, G., Langdon, M., Gelein, R., Weiss, B., 2010. Organic and inorganic mercury in neonatal rat brain after prenatal exposure to methylmercury and mercury vapor. *Environ. Health Perspect.* 118, 242–248.
- James, S.J., Slikker, W., Melnyk, S., New, E., Pogribna, M., Jernigan, S., 2005. Thimerosal neurotoxicity is associated with glutathione depletion: protection with glutathione precursors. *Neurotoxicology* 26, 1–8.
- Johnson, J.A., el Barbary, A., Kornguth, S.E., Brugge, J.F., Siegel, F.L., 1993. Glutathione-S-transferase isoenzymes in rat brain neurons and glia. *J. Neurosci.* 13, 2013–2023.
- Johnston, M.V., 2005. Excitotoxicity in perinatal brain injury. *Brain Pathol.* 15, 234–240.
- Kudo, A., Fujikawa, Y., Miyahara, S., Zheng, J., Takigami, H., Sugahara, M., Muramatsu, T., 1998. Lessons from minamata mercury pollution, Japan – after a continuous 22 years of observation. *Water Sci. Technol.* 38, 187–193.
- Letourneau, P.C., 2009. Actin in axons: stable scaffolds and dynamic filaments. *Results Probl. Cell Differ.* 48, 265–290.
- Li, P., Feng, X.B., Qiu, G.L., Shang, L.H., Li, Z.G., 2009. Mercury pollution in Asia: a review of the contaminated sites. *J. Hazard. Mater.* 168, 591–601.
- Marrs, K.A., 1996. The functions and regulation of glutathione S-transferases in plants. *Annu. Rev. Plant Physiol. Plant Mol. Biol.* 47, 127–158.
- Meldrum, B.S., 2000. Glutamate as a neurotransmitter in the brain: review of physiology and pathology. *J. Nutr.* 130, 1007–1015.
- Moncrief, N.D., Kretsinger, R.H., Goodman, M., 1990. Evolution of EF-hand calcium-modulated proteins: relationships based on amino acid sequences. *J. Mol. Evol.* 30, 522–562.
- Monteiro, D.A., Rantin, F.T., Kalinin, A.L., 2010. Inorganic mercury exposure: toxicological effects, oxidative stress biomarkers and bioaccumulation in the tropical freshwater fish matrinxã, *Brycon amazonicus* (Spix and Agassiz, 1829). *Ecotoxicology* 19, 105–123.
- Mousavi, A., Chávez, R.D., Ali, A.M.S., Cabanissa, S.E., 2011. Mercury in natural waters: a mini-review. *Environ. Forensics* 12, 14–18.
- Ni, M.W., Li, X., Yin, Z.B., Jiang, H.Y., Sidoryk-Wegrzynowicz, M., Milatovic, D., Cai, J.Y., Aschner, M., 2010. Methylmercury induces acute oxidative stress, altering Nrf2 protein level in primary microglial cells. *Toxicol. Sci.* 116, 590–603.
- Nylander, M., Weiner, J., 1991. Mercury and selenium concentrations and their interrelations in organs from dental staff and the general population. *Br. J. Ind. Med.* 48, 729–734.
- Oliveira Ribeiro, A.O., Fanta, E., Turcatti, N.M., Cardoso, R.J., Carvalho, C.S., 1996. Lethal effects of inorganic mercury on cells and tissues of *Trichomycterus brasiliensis* (Pisces; Siluroidei). *Biocell* 20, 171–178.
- Ozawa, S., Kamiya, H., Tsuzuki, K., 1998. Glutamate receptors in the mammalian central nervous system. *Prog. Neurobiol.* 54, 581–618.
- Perottoni, J., Rodrigues, O.E.D., Paixao, M.W., Zeni, G., Lobato, L.P., Braga, A.L., Rocha, J.B.T., Emanuelli, T., 2004. Renal and hepatic ALA-D activity and selected oxidative stress parameters of rats exposed to inorganic mercury and organoselenium compounds. *Food Chem. Toxicol.* 42, 17–28.
- Pfeiffer, W.C., Lacerda, L.D., 1988. Mercury inputs in the Amazon region. *Environ. Technol. Lett.* 9, 325–330.
- Porciuncula, L.O., Rocha, J.B., Tavares, R.G., Ghisleni, G., Reis, M., Souza, D.O., 2003. Methylmercury inhibits glutamate uptake by synaptic vesicles from rat brain. *NeuroReport* 14, 577–580.
- Radyuk, S.N., Klitchko, V.I., Spinola, B., Sohal, R.S., Orr, W.C., 2001. The peroxiredoxin gene family in *Drosophila melanogaster*. *Free Radic. Biol. Med.* 31, 1090–1100.
- Rana, S.V.S., 2008. Metals and apoptosis: recent developments. *J. Trace Elem. Med. Biol.* 22, 262–284.
- Risher, J.F., De Rosa, C.T., 2007. Inorganic: the other mercury. *J. Environ. Health* 70, 9–16.
- Roland, K., Kestemont, P., Hénuset, L., Pierrard, M.A., Raes, M., Dieu, M., Silvestre, F., 2013. Proteomic responses of peripheral blood mononuclear cells in the European eel (*Anguilla anguilla*) after perfluorooctane sulfonate exposure. *Aquat. Toxicol.* 128–129, 43–52.
- Sakai, J., Li, J., Subramanian, K.K., Mondal, S., Bajrami, B., Hattori, H., Jia, Y., Dickinson, B.C., Zhong, J., Ye, K., Chang, C.J., Ho, Y.S., Zhou, J., Luo, H.R., 2012. Reactive oxygen species-induced actin glutathionylation controls actin dynamics in neutrophils. *Immunity* 37, 1037–1049.
- Sheehan, D., Crimmins, K.M., Burnell, G.M., 1991. Evidence for glutathione S-transferase activity in *Mytilus edulis* as an index of chemical pollution in marine estuaries, in: Jeffrey, D.W., Maden, B. (Eds.), *Bioindicators and Environmental Management*. London, pp. 419–425.
- Siegel, G.J., Albers, R.W., Brady, S.T., Price, D.L., 2006. *Basic Neurochemistry: Molecular, Cellular, and Medical Aspects*, seventh ed. Elsevier Academic Press, Amsterdam.
- Tannu, N.S., Hemby, S.E., 2006. Two-dimensional fluorescence difference gel electrophoresis for comparative proteomics profiling. *Nat. Protoc.* 1, 1732–1742.
- Ung, C.Y., Lam, S.H., Hlaing, M.M., Winata, C.L., Korzh, S., Mathavan, S., Gong, Z., 2010. Mercury-induced hepatotoxicity in zebrafish: in vivo mechanistic insights from transcriptome analysis, phenotype anchoring and targeted gene expression validation. *BMC Genom.* 11, 212–227.
- Vahter, M.E., Mottet, N.K., Friberg, L.T., Lind, S.B., Charleston, J.S., Burbacher, T.M., 1995. Demethylation of methyl mercury in different brain sites of *Macaca fascicularis* monkeys during long-term subclinical methylmercury exposure. *Toxicol. Appl. Pharmacol.* 134, 273–284.
- Virtanen, J., Rissanen, T., Voutilainen, S., Tuomainen, T., 2007. Mercury as a risk factor for cardiovascular disease. *J. Nutr. Biochem.* 18, 75–85.
- Walsh, C.T., 1982. The influence of age on the gastrointestinal absorption of mercury chloride and methyl mercury chloride in the rat. *Environ. Res.* 27, 412–420.
- Wang, M., Chan, L.L., Si, M., Hong, H., Wang, D., 2010. Proteomic analysis of hepatic tissue of zebrafish (*Danio rerio*) experimentally exposed to chronic microcystin-LR. *Toxicol. Sci.* 113, 60–69.
- Wang, M., Wang, Y., Wang, J., Lin, L., Hong, H., Wang, D., 2011. Proteome profiles in medaka (*Oryzias melastigma*) liver and brain experimentally exposed to acute inorganic mercury. *Aquat. Toxicol.* 103, 129–139.
- Yasutake, A., Sawada, M., Shimada, A., Satoh, M., Tohyama, C., 2004. Mercury accumulation and its distribution to metallothionein in mouse brain after sub-chronic pulse exposure to mercury vapor. *Arch. Toxicol.* 78, 489–495.
- Zalups, R.K., 2000. Molecular interactions with mercury in the kidney. *Pharmacol. Rev.* 52, 113–143.
- Zheng, W., Aschner, M., Ghersi-Egea, J.F., 2003. Brain barrier systems: a new frontier in metal neurotoxicological research. *Toxicol. Appl. Pharmacol.* 192, 1–11.